Struct Multidisc Optim (2008) 36:143–158
DOI 10.1007/s00158-007-0205-4

RESEARCH PAPER

Analytical benchmarks for topological optimization IV: square-shaped line support

T. Lewiński · G. I. N. Rozvany

Received: 7 September 2007 / Accepted: 9 October 2007 / Published online: 12 January 2008
© Springer-Verlag 2007

Abstract Michell's problem of optimizing truss topology for stress or compliance constraints under a single load condition is solved analytically for plane trusses having a square-shaped line support. Geometrical characteristics of the Hencky nets giving the truss layout are expressed in terms of Lommel functions. Analytically derived truss volumes for the above problem are compared with those of trusses supported along circles of equivalent area. Some general implications of the results are also discussed.

Keywords Michell trusses · Optimal truss layout · Topology optimization · Lommel functions · Stress constraints

1 Introduction

The paper deals with plane Michell trusses transmitting given point loads outside a given square-shaped line support. The limit stresses in tension and compression are set to be equal. The present study is an extension of the results in papers by Lewiński et al. (1994a, b), Rozvany (1998) and Lewiński and Rozvany (2007, 2008). Optimality criteria for Michell trusses and methods for deriving an exact solution were summarized by Lewiński and Rozvany (2007).

Numerical solutions by a level set method for the considered class of problems were obtained by Allaire and Jouve (2006).

For the longest distance of a point load $\boldsymbol{P}$ from the square support, for which the solution is derived in this paper, the exact optimal truss layout is shown in Fig. 1.

T. Lewiński (✉)
Faculty of Civil Engineering, Institute of Structural Mechanics,
Warsaw University of Technology,
al. Armii Ludowej 16,
00-637 Warsaw, Poland
e-mail: T.Lewinski@il.pw.edu.pl

G. I. N. Rozvany
Department Structural Mechanics,
Budapest University of Technology and Economics,
Müegyetem rkp.3, Kmf.35,
1521 Budapest, Hungary
e-mail: smo.rozvany@t-online.hu

2 General implications of the solutions presented

2.1 Admissible load directions and superposition principle

As in several other papers of the authors, the optimal layouts in this paper are valid, if out of the two truss members intersecting at that load, one is in tension and the other one in compression. This can be verified by a simple force diagram (see Fig. 2a, in which "+" indicates tension and "–" denotes compression.

Moreover, the same layout is valid for any number of simultaneous loads, if (1) they are oriented in accordance with the above rule and (2) in any given member they all cause forces of the same sign. Some admissible point loads and distributed loads are shown in Fig. 2b.

2.2 Concentrated and distributed members in Michell trusses

In Michell trusses for point loads, we usually have concentrated and "distributed" members. Prager and Rozvany (1977) called such structures "truss-like continua". For a single point load $\boldsymbol{P}$, prismatic concentrated members (of constant cross-sectional area) occur along the bound-

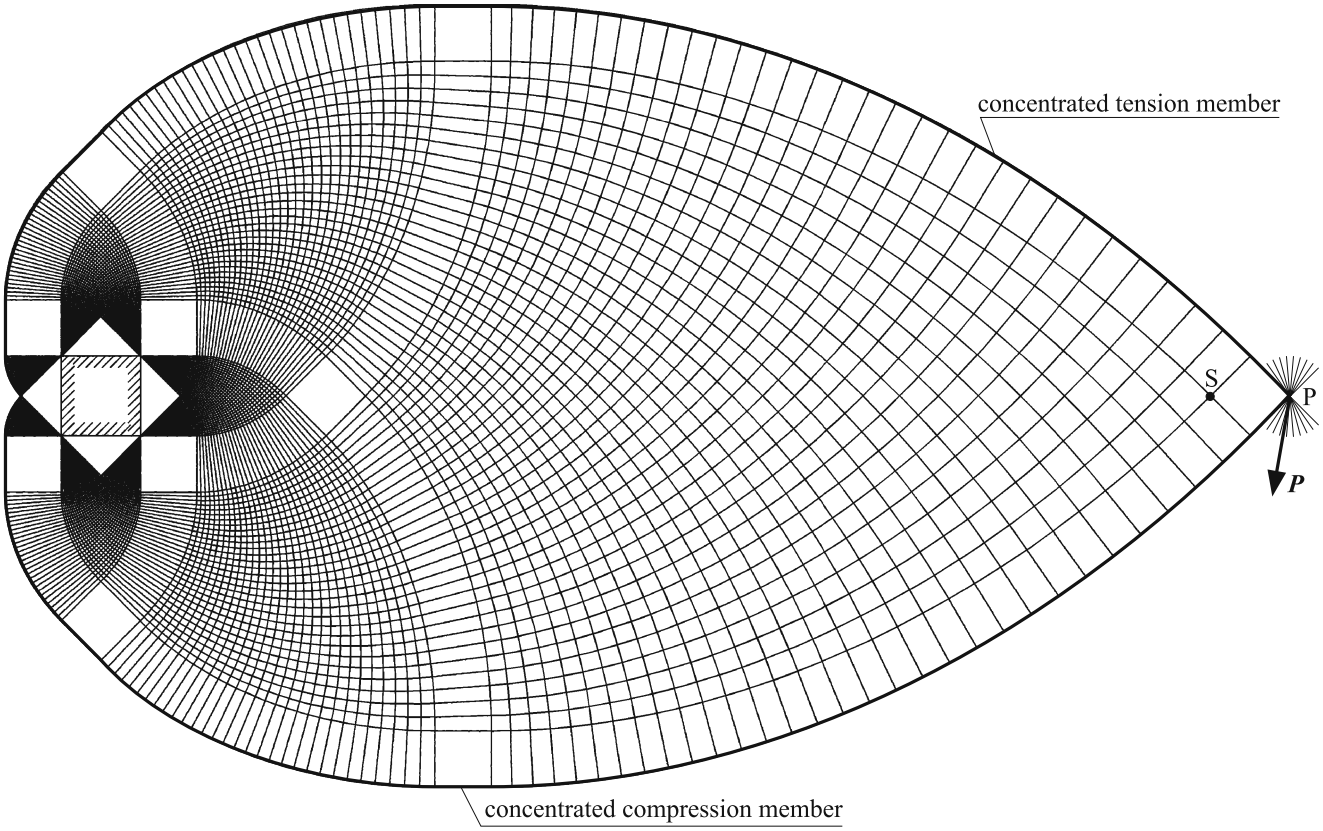

Fig. 1 The longest cantilever considered. Force ***P*** must be directed within the fans indicated

aries of the layout in Fig. 1 (indicated by thicker lines). However, no concentrated members occur, if only distributed loads act on the same structure.

"Distributed members" have an infinitesimal spacing and infinitesimal cross-sectional area, but their density per unit width is usually finite and varying. In Fig. 1, their density takes on an infinite value only at the corners of the square support, where an infinite number of distributed members from a circular fan meet. Distributed members can also be visualized as prismatic "fibers" (of constant cross-sectional area), whose spacing varies along the structure.

2.3 Primal and dual method for calculating truss volumes

The density of the distributed members is integrable. Integration gives the material volume of the distributed members. To derive the total volume by the "primal" method, the volume of concentrated members must be added to this. This method is fairly laborious, it was performed for another class of problems by Graczykowski and Lewiński (2005, 2006, 2007).

As noted already by Michell (1904), the total truss volume may also be calculated from the virtual work of the external load(s), that is, from the product of the loads and the "adjoint" displacement(s) at (and in the direction) of the loads. Michell's problem is actually "self-adjoint", so that real strains along nonvanishing members are proportional to the adjoint strains along the same lines. For further explanations, see the paper by Lewiński and Rozvany (2007), Sections 2 through 5.

2.4 Multi-region Michell topologies

Most of the published Michell truss solutions have relatively few "regions" (subsets of the design domain, for which the adjoint strain fields and member geometry is described by a single set of equations). This applies particularly to solutions derived by the Hemp group (e.g., Hemp 1973). In the simple illustrative example in Section 4, Lewiński and Rozvany (2007), we had only two optimal regions.

The solution in Fig. 1 consists of 40 regions, namely (a) 14 (square or triangular) regions with orthogonal straight trajectories (lines of principal strains), (b) 20 regions having straight trajectories in one direction only, and (c) 6 regions having only curved, orthogonal trajectories.

In Fig. 1, there are no members on the interior of the square and triangular regions with straight trajectories, if we consider only the load ***P*** as indicated. However, this is not necessarily so if loads are applied elsewhere (for example somewhere along the line segment PS in Fig. 1).

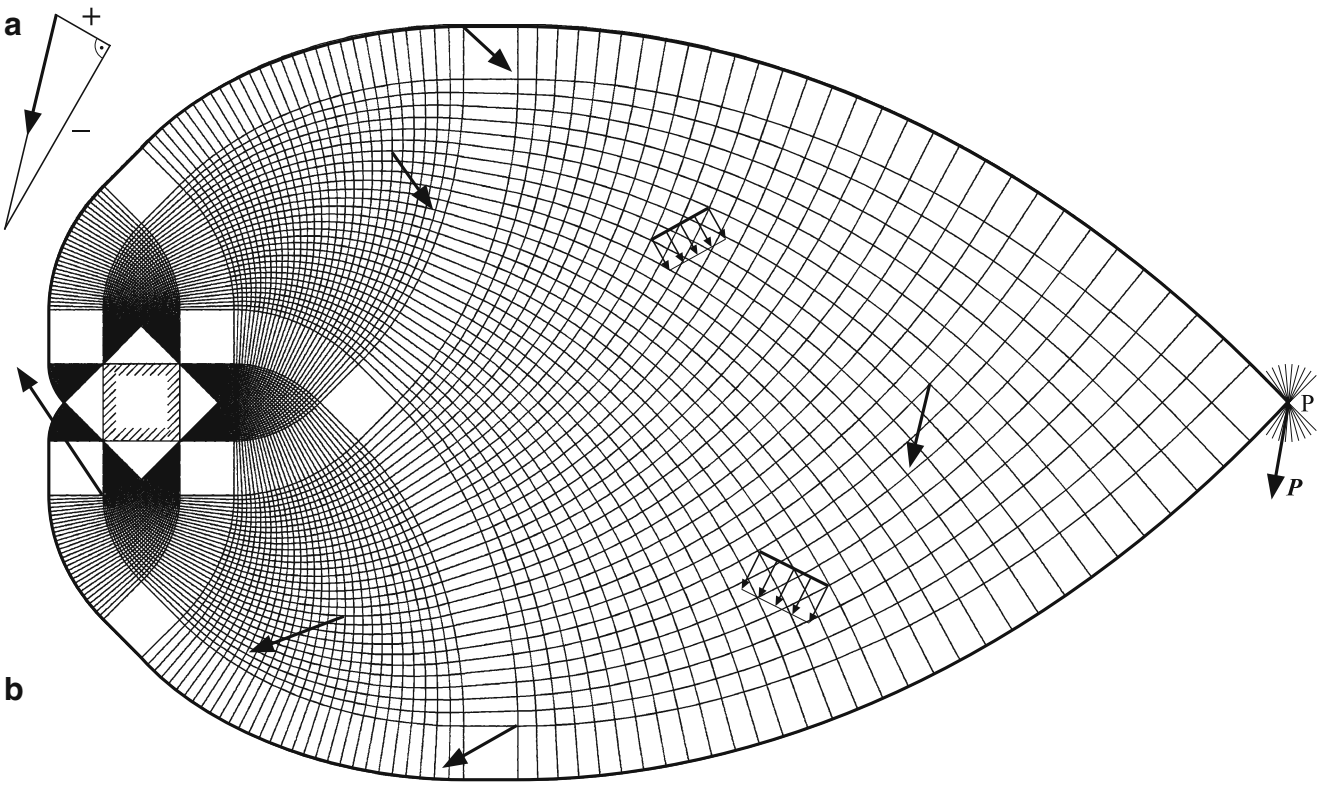

Fig. 2 Admissible simultaneous loads for the optimal layout in Fig. 1

2.5 Loads inside a square support

This class of problems was fully solved earlier, see Rozvany and Gollub (1990) and Rozvany et al. (1997). For this class of problems, at least one optimal layout consists of one or two bars, although some others with the same volume may have more. Moreover, the number of optimal regions is usually four or less. Some very simple illustrative solutions are shown in Fig. 3.

Figure 3a shows the optimal Michell layouts for vertical point loads inside a square-shaped support. In the two side-regions, the solution consists of two bars at ±45 degrees to the vertical. In the central regions, the optimal layout consists of a single vertical bar. For comparison, an optimal truss layout is shown for a vertical load outside the square support, which is similar to the ones in the two side-regions inside, but the region boundary for its validity is at 1:1, instead of 1:2.

Figure 3b shows the optimal Michell layout for a point load along the diagonal of the square-shaped line support. The above papers actually give analytical expressions for a point load inside the square in any location and any direction.

The second paper describes also a computer program for deriving analytically the optimal Michell layout for a point load inside any convex polygonal boundary.

2.6 Cognitive procedure for deriving exact optimal topologies

As noted earlier (Lewiński and Rozvany 2007), the derivation of a complex new optimal topology requires two cognitive stages. First, the topology of the optimal regions must be guessed correctly, which (in terms of cognitive psychology) requires "intuition", "creative thinking", or "insight", i.e., cannot be done by deductive reasoning. Second, the exact geometry needs to be determined quantitatively for the guessed region topology, showing that the assumed solution does satisfy all optimality criteria. The second stage is a deductive procedure, but extremely laborious, requiring advanced mathematical treatment. The above procedure was illustrated on a simple example in the above-cited paper, but the effort required for more advanced examples is considerably greater.

The first "intuitive" stage of the above cognitive procedure can be helped by discretized numerical solutions. For example, in deriving the exact analytical solution for the "MBB beam" in Lewiński et al. (1994b), for the region topology Zhou's numerical solutions with the SIMP method have given a clue. However, the exact solutions in the current paper are too complicated for guessing them on the basis of a discretized layout by presently available numerical methods and computer capabilities.

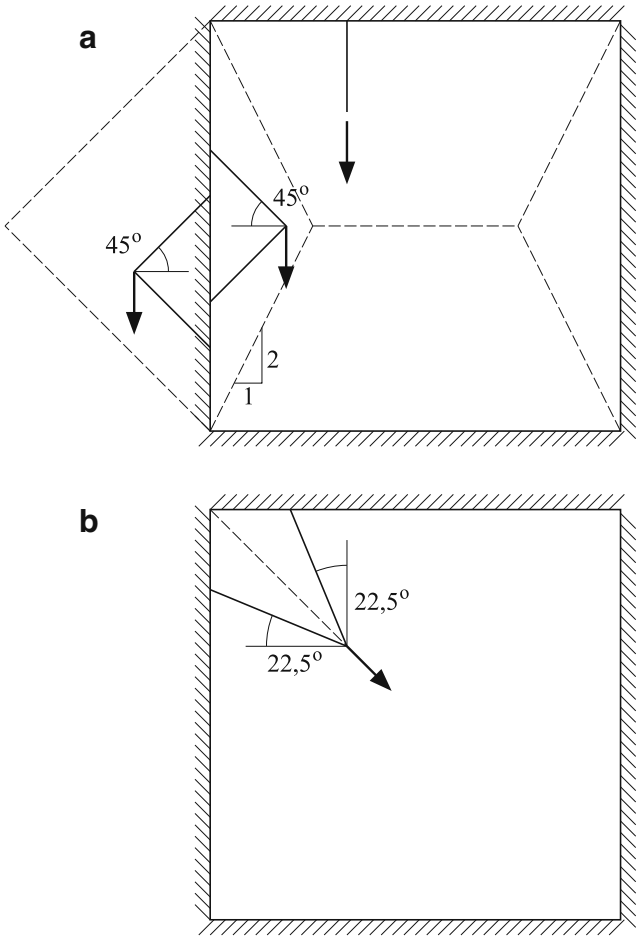

Fig. 3 Loads inside a square support

The region topology of the solution in Fig. 1 was correctly guessed by the second author more than a decade ago (Rozvany et al. (1995), conference presentation 1993; diagram repeated in Fig. 4 of Lewiński and Rozvany 2007).

For this region topology, the exact optimal geometry was derived by the first author, taking advantage of the fact that the considered solution consists of only so-called "T-regions" (see section 2 of Lewiński and Rozvany 2007). In this type of regions, the two principal strains have opposite signs but constant magnitude and form so-called Hencky nets, which are well known from the theory of plasticity. They can be derived by satisfying continuity of the adjoint displacements along region boundaries and kinematic support conditions. The derivations are so extensive that much detail had to be left out of this paper but can be obtained from the first author.

It is to be remarked that once a number of exact analytical solutions have been derived for a certain class of load and support conditions, it is possible to observe some regular features of these solutions and to construct a method for deriving systematically solutions for the entire class of problems, even by computer. As mentioned, such a program was developed for nonnumeric derivation of optimal truss topologies for a point load inside any convex polygonal line support (Rozvany et al. 1997). Investigation of exact optimal grillages (beam systems) progressed much further already some 20 years ago, making it possible to derive the optimal topology in a closed analytical form (even by computer) for almost any support and load condition. For a brief overview, see the review article by Rozvany et al. (1995).

3 Conventions adopted for referring to earlier publications

For the sake of brevity the equation of number (N) of Lewiński et al. (1994a) will be referred to as Eq. (a.N). We shall frequently use mathematical results of section 2 of the above-mentioned paper and of appendices to this paper and to Graczykowski and Lewiński (2006, part I), without specifically mentioning this. To make the paper possibly compact, almost all details of the analytical derivations are omitted. The results will be expressed in terms of the functions: $G_n(\alpha, \beta)$ and $F_n(\alpha, \beta)$, see Eqs. (a.1, a.2), with integer indices n. They will be called Chan's functions to honor H.S.Y. Chan's (1963, 1964, 1967, 1975) publications, which paved the way for further progress. The equation (N) [or Fig. M] of Part II or Part III, or of Lewiński and Rozvany (2007, 2008) will be referred to as Eq. (II.N) or Eq. (III.N) [Fig. II.M, Fig. III.M] for brevity.

The following new functions will be used to shorten notation:

$$T_n(\alpha, \beta) = G_n(\alpha, \beta) + G_{n+1}(\alpha, \beta)$$
$$H_n(\alpha, \beta) = F_n(\alpha, \beta) + F_{n+1}(\alpha, \beta) \tag{3.1}$$

The points like P, R, B, A, N will be printed as straight fonts, while the mathematical symbols, like functions $A(\alpha, \beta)$, $B(\alpha, \beta)$ will be printed in italic. The force $\boldsymbol{P}$ has magnitude P and is applied at point P.

The notation used follows that of Hemp (1973), Chan (1967), Lewiński et al. (1994a) and Lewiński and Rozvany (2007, 2008).

4 Lamé coefficients for Hencky nets in optimal domains

The Hencky net for the exterior of the square E_3RNC_3 is described in Fig. 4. The square dimensions are: $|RN| = a, |RE_3| = a, |TR| = r,\ r = a\sqrt{2}/2$ or $a = \sqrt{2}r$.

In the first step, we shall find the Lamé coefficients A and B in the regions depicted in Fig. 4. The regions RAN,

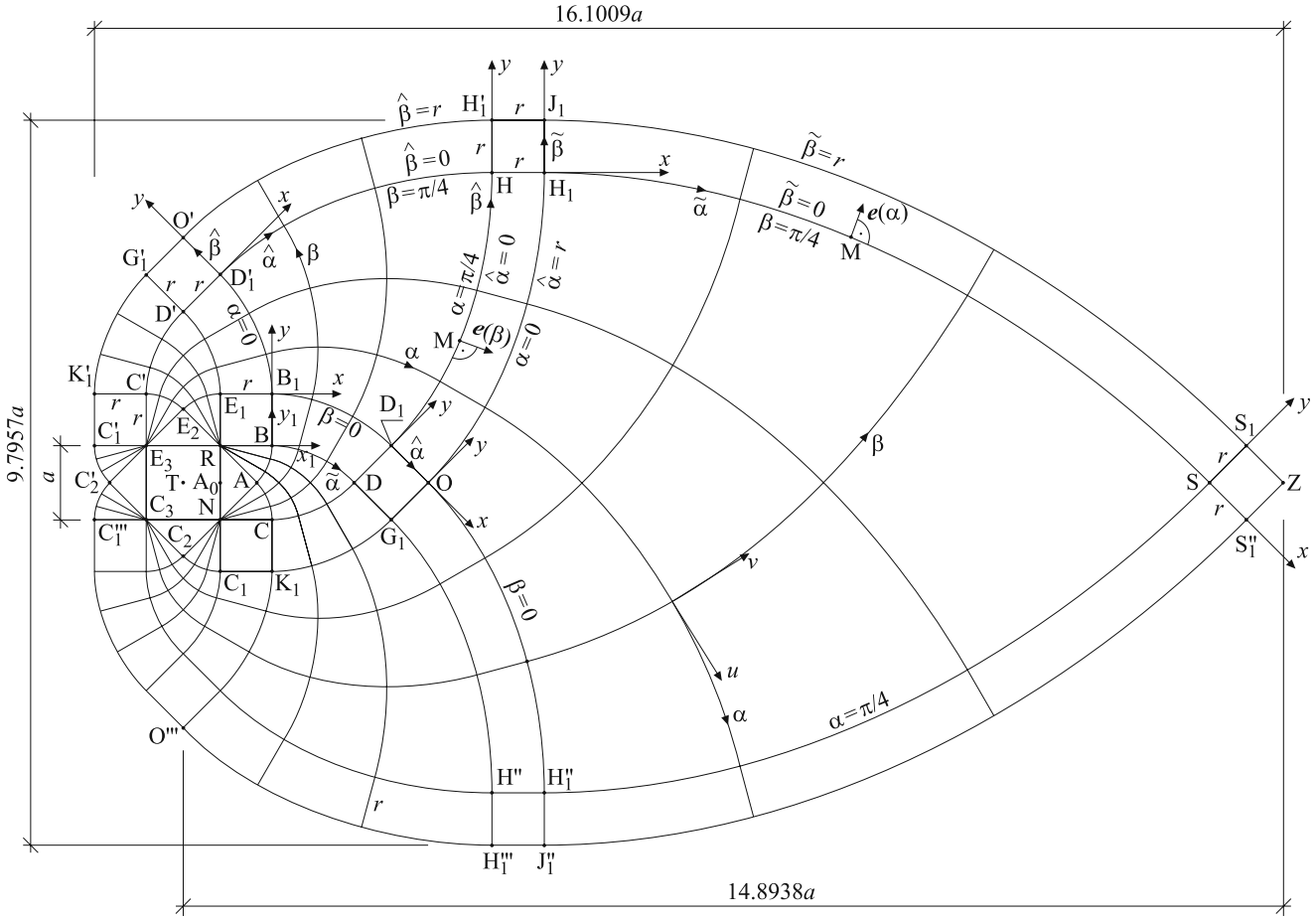

Fig. 4 Parameterization of the Hencky net

RBA, NAC, ABDC, BB_1D_1D, RBB_1E_1, DD_1OG_1, RE_1E_2, RE_2E_3 have been analyzed in Lewiński and Rozvany (2007, 2008), and all the analytical formulae for A and B were found there. Our aim here is to extend these results to the further domains.

4.1 Domain $B_1D_1HD_1'$

The Hencky net is based on two curves: B_1D_1 and B_1D_1'. We introduce (α, β) coordinates within $B_1D_1HD_1'$ such that B_1 has coordinates (0,0), B_1D_1 is the α-line with β=0, and B_1D_1' is the β-line with α=0.

The fibers along the β lines will be in compression. Since both α and β lines are curved, we have here: $\phi(\alpha, \beta)=\beta-\alpha$ where the angle ϕ, see Hemp (1973), is referred to the x-axes of the (x,y) frame of origin at B_1. Inclination of D_1O shows that $\phi = -\pi/4$ at D_1. Thus $\alpha = \pi/4$ along D_1H and $\beta = \pi/4$ along $D_1'H$, by symmetry with respect to the B_1H axis.

The Lamé fields A (α, β), $B(\alpha, \beta)$ in the domain $B_1D_1HD_1'$ satisfy the equations (a.51, a.52). They will be found by using Riemann's formula (a.17). It has the following form for A at (λ, μ)

$$A(\lambda, \mu) = A(0, 0)G_0(\lambda, \mu)+ + \int_0^{\lambda} G_0(\lambda-\alpha, \mu)\frac{\partial A(\alpha, 0)}{\partial \alpha}d\alpha+ + \int_0^{\mu} G_0(\lambda, \mu-\beta)\frac{\partial A(0, \beta)}{\partial \beta}d\beta \qquad (4.1)$$

where $G_0(\lambda, \mu)$ is given by Eq. (a.1). Since $\partial A(0,\beta)/\partial\beta = B(0,\beta)$ we should recall the formulae for A $(\alpha, 0)$ and B $(0, \beta)$ found in Lewiński and Rozvany (2007). We note that A is continuous along B_1D_1 and B–along B_1D_1'. By using the results from the paper above one obtains

$$\frac{A(\alpha,0)}{r} = 1 + T_0\left(\frac{\pi}{4}, \alpha\right)$$
$$\frac{B(0,\beta)}{r} = 1 + T_0\left(\frac{\pi}{4}, \beta\right) \qquad (4.2)$$

where T_0=T_n for n=0, see (3.1). We note that $A(0,0) = \left(2+\frac{\pi}{4}\right)r$. Substitution of (4.2) into (4.1) and appropriate integration gives

$$\frac{A(\lambda,\,\mu)}{r} = T_0\left(\mu+\frac{\pi}{4},\,\lambda\right) + T_0\left(\mu,\,\lambda+\frac{\pi}{4}\right) \tag{4.3}$$

$$B(\lambda,\,\mu) = A(\mu,\,\lambda) \tag{4.4}$$

It is easy to check that the formulae above satisfy the field equations (a.51, a.52) and the boundary conditions (4.2). It is much easier to guess the results (4.3, 4.4) than to derive them.

4.2 Domain $D_1'HH_1'O'$

The results (4.3, 4.4) will be extended into the domain $D_1'HH_1'O'$ through the line $D_1'H$, where $\beta=\pi/4$. We introduce the coordinate system $(\hat{\alpha},\hat{\beta})$ within $D_1'HH_1'O'$ such that the $\hat{\beta}=0$ line coincides with the $\beta=\pi/4$ line and there $\hat{\alpha}=\alpha$. The $\hat{\beta}$ lines (or $\hat{\alpha}=const$) are straight. Let $A(\hat{\alpha},\hat{\beta})$, $B(\hat{\alpha},\hat{\beta})$ represent Lamé fields in the domain considered. We see that B=1, provided that $\hat{\beta}$ measures a distance from the $D_1'H$ line, such that $\hat{\beta}=r$ along $O'H'_1$. Since the $\hat{\beta}$ lines are straight, we note that $\phi=-\hat{\alpha}$ with respect to the (x,y) Cartesian coordinate system at origin at D_1'.

Thus $\frac{\partial A\left(\hat{\alpha},\hat{\beta}\right)}{\partial\hat{\beta}}=1$, hence $A\left(\hat{\alpha},\hat{\beta}\right)=\hat{\beta}+f_1(\hat{\alpha})$ and $f_1\left(\hat{\alpha}\right)=A\left(\hat{\alpha},\hat{\beta}=0\right)$. We recall that A is continuous along $D_1'H$, which implies $f_1(\widehat{\alpha})=A\left(\widehat{\alpha},\frac{\pi}{4}\right)$, where A is given by (4.3). We eventually find

$$\begin{aligned} A\left(\hat{\alpha},\,\hat{\beta}\right) &= \hat{\beta}+r\left[T_0\left(\tfrac{\pi}{2},\,\hat{\alpha}\right)+T_0\left(\tfrac{\pi}{4},\,\hat{\alpha}+\tfrac{\pi}{4}\right)\right] \\ B\left(\hat{\alpha},\,\hat{\beta}\right) &= 1 \end{aligned} \tag{4.5}$$

4.3 Domain D_1HH_1O

The Hencky net is symmetric with respect to B_1H line, which implies the following formulae for $A\left(\hat{\alpha},\hat{\beta}\right)$, $B\left(\hat{\alpha},\hat{\beta}\right)$ within the domain D_1HH_1O, parameterized by the coordinate system $\left(\hat{\alpha},\hat{\beta}\right)$, as shown in Fig. 4

$$\begin{aligned} A\left(\hat{\alpha},\,\hat{\beta}\right) &= 1 \\ B\left(\hat{\alpha},\,\hat{\beta}\right) &= \hat{\alpha}+r\left[T_0\left(\tfrac{\pi}{2},\,\hat{\beta}\right)+T_0\left(\tfrac{\pi}{4},\,\hat{\beta}+\tfrac{\pi}{4}\right)\right] \end{aligned} \tag{4.6}$$

We note that $\hat{\beta}=\beta$ along D_1H, where α=0 and $\hat{\alpha}=0$. Along OH_1, where $\hat{\alpha}=r$ we have $B=B\left(r,\hat{\beta}\right)$, with $B(\cdot,\cdot)$ given by (4.6). The net within $OH''_1H''G_1$ is constructed by symmetry with respect to the OS axis, hence the details can be omitted.

4.4 Domain OH_1SH_1''

We introduce the parametric lines (α, β), both curved, such that $\phi=\beta-\alpha$ with respect to the (x,y) frame of origin at O. Along OH_1 $\widehat{\alpha}=r$ and now α=0. Along OH_1'' we have β=0. We note that $\alpha=\pi/4$ at H_1, hence $\beta=\pi/4$ along H_1S and $\alpha=\pi/4$ along $H_1''S$. By symmetry with respect to OS we write the formula for A along OH_1''

$$\frac{A(\alpha,\,0)}{r} = 1+T_0\left(\frac{\pi}{2},\,\alpha\right)+T_0\left(\frac{\pi}{4},\alpha+\frac{\pi}{4}\right) \tag{4.7}$$

The field B along OH_1 is given by B (0, β)=A(β, 0) with A(β, 0) given by (4.7). We recall that $\frac{\partial A(0,\beta)}{\partial\beta}=B(0,\beta)$ and use (4.1). Now the integration is much more complex than previously. We use the available integration formulae of Lewiński et al. (1994a) and from the Appendix of the present paper. In particular, the formulae (A.5–A.7) are applied for S=G, n=0, n=1. Rather lengthy derivation gives

$$\begin{aligned} A(\lambda,\,\mu) &= T_0\left(\mu+\tfrac{\pi}{4},\lambda+\tfrac{\pi}{4}\right)+T_0\left(\mu,\,\lambda+\tfrac{\pi}{2}\right)+ \\ &\quad +T_0\left(\mu+\tfrac{\pi}{2},\,\lambda\right) \\ B(\lambda,\,\mu) &= A(\mu,\,\lambda) \end{aligned} \tag{4.8}$$

One can verify that A, B satisfy (a.51) and the boundary conditions along β=0 and α=0. This confirms (4.8), since such fields A, B are uniquely determined.

4.5 Domain $H_1SS_1J_1$

We introduce the parameterization $\left(\widetilde{\alpha},\widetilde{\beta}\right)$ such that $\widetilde{\beta}=0$ is equivalent to $\beta=\pi/4$, the $\widetilde{\beta}$ lines are straight such that $\phi=-\widetilde{\alpha}$ with respect to (x,y) frame of origin at H_1. The boundary line J_1S_1 is given by $\widetilde{\beta}=r$. Thus $B\left(\widetilde{\alpha},\widetilde{\beta}\right)=1$. We use: $\frac{\partial A\left(\widetilde{\alpha},\widetilde{\beta}\right)}{\partial\widetilde{\beta}}=1$ and recall the boundary condition: $A(\widetilde{\alpha},0)=A(\widetilde{\alpha},\beta=\pi/4)$, where the latter function $A(\cdot,\cdot)$ is defined by (4.8). This yields

$$\begin{aligned} A\left(\widetilde{\alpha},\widetilde{\beta}\right) &= \widetilde{\beta}+r\left[T_0\left(\tfrac{\pi}{2},\widetilde{\alpha}+\tfrac{\pi}{4}\right)+\right. \\ &\quad \left.+T_0\left(\tfrac{\pi}{4},\widetilde{\alpha}+\tfrac{\pi}{2}\right)+T_0\left(\tfrac{3}{4}\pi,\widetilde{\alpha}\right)\right], \\ B\left(\widetilde{\alpha},\widetilde{\beta}\right) &= 1 \end{aligned} \tag{4.9}$$

The Lamé fields within other domains of Fig. 4 can be constructed by symmetry or refer to Cartesian frames, as in $HH_1J_1H_1'$, for instance.

5 Virtual displacement fields

The virtual displacement fields (u,v) within RAN, RBA, NAC, ABDC, BB_1D_1D, BB_1E_1R, RE_1E_2, E_2E_3R have been constructed in Lewiński and Rozvany (2007). One should put $\gamma=\pi/2$ and $\theta=\pi/4$ into all reported results.

The virtual displacements (u,v) within $B_1D_1'D'E_1$ can be constructed by antisymmetric reflection with respect to the B_1H axis. Thus, the first new problem concerns:

5.1 Domain $B_1D_1HD_1'$

This domain is parameterized by (α, β) and by (x,y) with origin at B_1. To find $u\ (\alpha, \beta)$ and $v\ (\alpha, \beta)$ we follow the idea proposed in Sec. 3 of Lewiński et al. (1994a). We construct the auxiliary fields $u^0\ (\alpha, \beta)$, $v^0\ (\alpha, \beta)$ satisfying

$$\frac{\partial^2 u^0}{\partial\alpha\partial\beta} - u^0 = 0, \quad \frac{\partial^2 v^0}{\partial\alpha\partial\beta} - v^0 = 0 \tag{5.1}$$

and the boundary conditions along the β=0 and α=0 lines:

$$\begin{aligned} u^0(\alpha, 0) &= u(\alpha, 0) - 2\alpha B(\alpha, 0) \\ u^0(0, \beta) &= u(0, \beta) \\ v^0(\alpha, 0) &= v(\alpha, 0) \\ v^0(0, \beta) &= v(0, \beta) + 2\beta B(0, \beta) \end{aligned} \tag{5.2}$$

The value $v^0\ (\lambda, \mu)$ is given by Riemann's formula (4.1) or

$$\begin{aligned} v^0(\lambda, \mu) = v^0(0, 0)G_0(\lambda, \mu) + \\ + \int_0^\lambda G_0(\lambda - \alpha, \mu)\frac{\partial v^0(\alpha, 0)}{\partial\alpha}d\alpha + \\ + \int_0^\mu G_0(\lambda, \mu - \beta)\frac{\partial v^0(0, \beta)}{\partial\beta}d\beta \end{aligned} \tag{5.3}$$

and the formula for $u^0\ (\lambda, \mu)$ is similar. Upon finding (u^0, v^0) we construct (u,v) by Eqs (a.66):

$$\begin{aligned} u^0(\alpha, \beta) &= u(\alpha, \beta) - 2\alpha A(\alpha, \beta) \\ v^0(\alpha, \beta) &= v(\alpha, \beta) + 2\beta B(\alpha, \beta) \end{aligned} \tag{5.4}$$

By antisymmetry of (u,v) along B_1H axis it is sufficient to find $v^0\ (\alpha, \beta)$ and then predict: $u^0\ (\alpha, \beta) = -v^0\ (\beta, \alpha)$.

We have also: $u(\alpha, \beta) = -v\ (\beta, \alpha)$

Thus to find $v^0\ (\lambda, \mu)$ within $B_1D_1HD_1'$, one should write down the boundary conditions along B_1D_1 and B_1D_1'.

By using the results of Lewiński and Rozvany (2007, 2008) one finds

$$\begin{aligned} \frac{v^0(\alpha, 0)}{r} &= -1 - \left(1 + \frac{\pi}{2}\right)G_0\left(\alpha, \frac{\pi}{4}\right) - \frac{\pi}{2}G_1\left(\alpha, \frac{\pi}{4}\right) \\ \frac{v^0(0, \beta)}{r} &= -1 - \frac{\pi}{2} - G_0\left(\beta, \frac{\pi}{4}\right) \end{aligned} \tag{5.5}$$

Note that $v^0(0,0) = -2 - \pi/2$. We substitute these results into (5.3), use appropriate differentiation and integration rules reported in Lewiński et al. (1994a) and Graczykowski and Lewiński (2006) to arrive at

$$\begin{aligned} \frac{v^0(\lambda, \mu)}{r} = -\left(1 + \tfrac{\pi}{2}\right)G_0\left(\lambda, \mu + \tfrac{\pi}{4}\right) + \\ -G_0\left(\mu, \lambda + \tfrac{\pi}{4}\right) - \tfrac{\pi}{2}G_1\left(\lambda, \mu + \tfrac{\pi}{4}\right) \end{aligned} \tag{5.6}$$

To find $v\ (\lambda, \mu)$ we should use $(5.4)_2$ and expression (4.4) for $B\ (\lambda, \mu)$. Moreover, $u(\lambda, \mu) = -v(\mu, \lambda)$. The rigid rotation reads

$$\omega(\alpha, \beta) = \omega(0, 0) - 2(\alpha + \beta) \tag{5.7}$$

where $\omega(0,0) = \omega(B_1) = -1 - \pi/2$, see section 7 in Lewiński and Rozvany (2007).

5.2 Domain $D_1'HH_1O'$

Construction of the virtual displacements in this region is based upon different ideas than in the previous case. We should follow the lines of reasoning proposed by Chan (1963) and revisited in Sec. II.7. We start with rigid rotation. It is given here by

$$\omega\left(\widehat{\alpha}, \widehat{\beta}\right) = \omega\left(D_1'\right) - 2\widehat{\alpha} \tag{5.8}$$

where, by (5.7), $\omega\left(D_1'\right) = -1 - \pi$. To find (u, v) we apply Eqs (II.24)

$$\frac{\partial u}{\partial\widehat{\beta}} = -\omega\left(\widehat{\alpha}, \widehat{\beta}\right), \quad \frac{\partial v}{\partial\widehat{\beta}} = -1 \tag{5.9}$$

with $\omega\left(\widehat{\alpha}, \widehat{\beta}\right)$ given by (5.8). Integration gives

$$\begin{aligned} u\left(\widehat{\alpha}, \widehat{\beta}\right) &= (1 + \pi + 2\widehat{\alpha})\widehat{\beta} + f_2(\widehat{\alpha}), \\ v\left(\widehat{\alpha}, \widehat{\beta}\right) &= -\widehat{\beta} + f_1(\widehat{\alpha}) \end{aligned} \tag{5.10}$$

where

$$f_1(\widehat{\alpha}) = v(\widehat{\alpha}, 0), \quad f_2(\widehat{\alpha}) = u(\widehat{\alpha}, 0) \tag{5.11}$$

The values of $u(\widehat{\alpha}, 0)$, $v(\widehat{\alpha}, 0)$, along $D_1'H$ can be found by continuity along this line, using (5.6), (5.4). This gives

$$\begin{aligned} \frac{u\left(\widehat{\alpha}, \widehat{\beta}\right)}{r} &= \frac{(1 + \pi + 2\widehat{\alpha})\widehat{\beta}}{r} + \\ &+ \left(1 + \frac{\pi}{2} + 2\widehat{\alpha}\right)G_0\left(\widehat{\alpha} + \frac{\pi}{4}, \frac{\pi}{4}\right) + \\ &+ (1 + 2\widehat{\alpha})G_0\left(\widehat{\alpha}, \frac{\pi}{2}\right) + 2\widehat{\alpha}G_1\left(\frac{\pi}{2}, \widehat{\alpha}\right) + \\ &+ \left(2\widehat{\alpha} + \frac{\pi}{2}\right)G_1\left(\frac{\pi}{4}, \widehat{\alpha} + \frac{\pi}{4}\right) \\ \frac{v\left(\widehat{\alpha}, \widehat{\beta}\right)}{r} &= -\frac{\widehat{\beta}}{r} - G_0\left(\widehat{\alpha}, \frac{\pi}{2}\right) - \pi G_0\left(\widehat{\alpha}, \frac{\pi}{2}\right) + \\ &- \left(1 + \frac{\pi}{2}\right)G_0\left(\frac{\pi}{4}, \widehat{\alpha} + \frac{\pi}{4}\right) + \\ &- \pi G_1\left(\widehat{\alpha}, \frac{\pi}{2}\right) - \frac{\pi}{2}G_1\left(\widehat{\alpha} + \frac{\pi}{4}, \frac{\pi}{4}\right) \end{aligned} \tag{5.12}$$

5.3 Domain D_1HH_1O

This domain is parameterized by $(\widehat{\alpha}, \widehat{\beta})$, see Fig. 4, such that $\widehat{\alpha} = r$ along OH_1, where $\widehat{\beta}$ varies from 0 on D_1O to $\pi/4$ on HH_1. Since the virtual displacement fields are antisymmetric with respect to B_1H, the results (5.12) are transformed to the form

$$\begin{aligned}\frac{u\left(\widehat{\alpha}, \widehat{\beta}\right)}{r} &= \frac{\widehat{\alpha}}{r} + G_0\left(\widehat{\beta}, \frac{\pi}{2}\right) + \pi G_0\left(\widehat{\beta}, \frac{\pi}{2}\right) + \\ &+ \left(1+\frac{\pi}{2}\right) G_0\left(\frac{\pi}{4}, \widehat{\beta}+\frac{\pi}{4}\right) + \\ &+ \pi G_1\left(\widehat{\beta}, \frac{\pi}{2}\right) + \frac{\pi}{2} G_1\left(\widehat{\beta}+\frac{\pi}{4}, \frac{\pi}{4}\right) \\ \frac{v\left(\widehat{\alpha}, \widehat{\beta}\right)}{r} &= -\frac{\left(1+\pi+2\widehat{\beta}\right)\widehat{\alpha}}{r} + \\ &- \left(1+\frac{\pi}{2}+2\widehat{\beta}\right) G_0\left(\widehat{\beta}+\frac{\pi}{4}, \frac{\pi}{4}\right) + \\ &- \left(1+2\widehat{\beta}\right) G_0\left(\widehat{\beta}, \frac{\pi}{2}\right) - 2\widehat{\beta} G_1\left(\frac{\pi}{2}, \widehat{\beta}\right) + \\ &- \left(2\widehat{\beta}+\frac{\pi}{2}\right) G_1\left(\frac{\pi}{4}, \widehat{\beta}+\frac{\pi}{4}\right)\end{aligned} \tag{5.13}$$

The rigid rotation is expressed by

$$\omega\left(\widehat{\alpha}, \widehat{\beta}\right) = -1 - \pi - 2\widehat{\beta} \tag{5.14}$$

and $\omega = -1-\pi$ at D_1. Note that behavior of ω is symmetric due to antisymmetry of the problem.

5.4 Domain $HH_1J_1H_1'$

Let this domain be parameterized by (x,y) frame with origin at H such that $y=0$ along HH_1 and $x=0$ along HH_1', see Fig. 4. Displacements *(u, v)* along (x,y) are expressed by (II.9) or by

$$u = x + C_1 y + D_1, \quad v = -y - C_1 x - D_1 \tag{5.15}$$

where

$$\begin{aligned} C_1 &= 1 + \tfrac{3}{2}\pi \\ \frac{D_1}{r} &= \left(2+\tfrac{3}{2}\pi\right) G_0\left(\tfrac{\pi}{4}, \tfrac{\pi}{2}\right) + \tfrac{\pi}{2} G_1\left(\tfrac{\pi}{2}, \tfrac{\pi}{4}\right) + \\ &+ \pi G_1\left(\tfrac{\pi}{4}, \tfrac{\pi}{2}\right)\end{aligned} \tag{5.16}$$

The field (u,v) is compatible with results (5.12, 5.13) along HH_1' and HH_1. The field ω is constant: $\omega = -1 - \frac{3}{2}\pi$.

5.5 Domain OH_1SH_1''

We use the Hencky net (α, β) such that $\alpha=0$ along OH_1, $\alpha=\pi/4$ along $H_1''S$, $\beta = 0$, $\beta=0$ along OH_1'' and $\beta=\pi/4$ along H_1S. Here $\phi = \beta - \alpha$, corresponding to (x,y) frame of origin at point O, see Fig. 4. Since $\omega(O) = -1 - \pi$, we have

$$\omega(\alpha, \beta) = -1 - \pi - 2(\alpha + \beta) \tag{5.17}$$

Knowing (u, v) and (A, B) along OH_1 and OH_1'' we can find v^0 along these lines

$$\begin{aligned}\frac{v^0(\alpha, 0)}{r} &= -1 - (1+\pi) G_0\left(\alpha, \frac{\pi}{2}\right) + \\ &- \left(1+\frac{\pi}{2}\right) G_0\left(\frac{\pi}{4}, \alpha+\frac{\pi}{4}\right) + \\ &- \pi G_1\left(\alpha, \frac{\pi}{2}\right) - \frac{\pi}{2} G_1\left(\alpha+\frac{\pi}{4}, \frac{\pi}{4}\right) \\ \frac{v^0(0, \beta)}{r} &= -(1+\pi) - \left(1+\frac{\pi}{2}\right) G_0\left(\beta+\frac{\pi}{4}, \frac{\pi}{4}\right) + \\ &- G_0\left(\beta, \frac{\pi}{2}\right) - \frac{\pi}{2} G_1\left(\frac{\pi}{4}, \beta+\frac{\pi}{4}\right)\end{aligned} \tag{5.18}$$

hence

$$\begin{aligned}\frac{v^0(0,0)}{r} &= -2 - \pi - \left(1+\frac{\pi}{2}\right) G_0\left(\frac{\pi}{4}, \frac{\pi}{4}\right) + \\ &- \frac{\pi}{2} G_1\left(\frac{\pi}{4}, \frac{\pi}{4}\right)\end{aligned} \tag{5.19}$$

To find $v(\lambda, \mu)$ at arbitrary point (λ, μ) of the domain OH_1SH_1' we apply the formula (5.3). We insert (5.18), use the differentiation rules (a.4) and the available integration rules, like e.g. (A7) to obtain $v^0(\alpha, \beta) = -u^0(\beta, \alpha)$,where

$$\begin{aligned}\frac{u^0(\alpha, \beta)}{r} &= (1+\pi) G_0\left(\beta, \alpha+\frac{\pi}{2}\right) + \\ &+ \left(1+\frac{\pi}{2}\right) G_0\left(\alpha+\frac{\pi}{4}, \beta+\frac{\pi}{4}\right) + \\ &+ \pi G_1\left(\beta, \alpha+\frac{\pi}{2}\right) + \\ &+ \frac{\pi}{2} G_1\left(\beta+\frac{\pi}{4}, \alpha+\frac{\pi}{4}\right) + G_0\left(\alpha, \beta+\frac{\pi}{4}\right)\end{aligned} \tag{5.20}$$

The fields *(u, v)* are given by (5.4), by the formulae above and by (4.8). They satisfy the required antisymmetry relation: $u(\alpha, \beta) = -v(\beta, \alpha)$.

5.6 Domain $H_1SS_1J_1$

This domain is parameterized by $(\widetilde{\alpha}, \widetilde{\beta})$ with origin at H_1 and by the Cartesian frame *(x, y)* with the same origin. Here $\phi\left(\widetilde{\alpha}, \widetilde{\beta}\right) = -\widetilde{\alpha}$, because the $\widetilde{\beta}$ lines are straight. The *(u, v)* fields are constructed the same way as in the domain D_1HH_1O'. We note that

$$\omega\left(\widetilde{\alpha}, \widetilde{\beta}\right) = -1 - \frac{3}{2}\pi - 2\widetilde{\alpha} \tag{5.21}$$

which is compatible with (5.17). Then we derive

$$\begin{aligned} u\left(\widetilde{\alpha}, \widetilde{\beta}\right) &= \left(1+\tfrac{3}{2}\pi + 2\widetilde{\alpha}\right)\widetilde{\beta} + u^0\left(\widetilde{\alpha}, \tfrac{\pi}{4}\right) + \\ &+ 2\widetilde{\alpha} A\left(\widetilde{\alpha}, \tfrac{\pi}{4}\right) \\ v\left(\widetilde{\alpha}, \widetilde{\beta}\right) &= -\widetilde{\beta} + v^0\left(\widetilde{\alpha}, \tfrac{\pi}{4}\right) - \tfrac{\pi}{2} B\left(\widetilde{\alpha}, \tfrac{\pi}{4}\right)\end{aligned} \tag{5.22}$$

where $u^0(\widetilde{\alpha},\pi/4)$, $A(\widetilde{\alpha},\pi/4)$, $v^0(\widetilde{\alpha},\pi/4)$, $B(\widetilde{\alpha},\pi/4)$ are values of the functions u^0 (α, β), $A(\alpha, \beta)$, $v^0(\alpha, \beta)$, $B(\alpha, \beta)$ corresponding to the domain OH_1SH_1'. Along the line SS_1 we have

$$\begin{aligned} u\left(\frac{\pi}{4},\widetilde{\beta}\right) &= (1+2\pi)\widetilde{\beta} + u^0\left(\frac{\pi}{4},\frac{\pi}{4}\right) + \frac{\pi}{2}A\left(\frac{\pi}{4},\frac{\pi}{4}\right) \\ v\left(\frac{\pi}{4},\widetilde{\beta}\right) &= -\widetilde{\beta} + v^0\left(\frac{\pi}{4},\frac{\pi}{4}\right) - \frac{\pi}{2}B\left(\frac{\pi}{4},\frac{\pi}{4}\right) \end{aligned} \tag{5.23}$$

with u^0, v^0, A, B referring to the OH_1SH_1'' domain.

5.7 Domain SS_1ZS_1''

The domain is parameterized by Cartesian frame (x, y) of origin at S, such that Z=Z(r, r). The displacements (u, v) are directed along (x, y) and are given by

$$u = x + C_1 y + D_1, \quad v = -y - C_1 x - D_1 \tag{5.24}$$

where

$$C_1 = 1 + 2\pi, \quad D_1 = u^0\left(\frac{\pi}{4},\frac{\pi}{4}\right) + \frac{\pi}{2}A\left(\frac{\pi}{4},\frac{\pi}{4}\right) \tag{5.25}$$

Here u^0, A refer to the OH_1SH_1'' domain. The rigid rotation is constant

$$\omega = -1 - 2\pi \tag{5.26}$$

We note that $u(x, y)=-v(y, x)$ due to antisymmetry.

6 Geometry of the Hencky net

Before deriving the volumes of Michell structures for the considered class of problems, we shall discuss the description of parametric lines α=const and β=const, including coordinates of nodal points, like D_1, H, ..., Z.

We have introduced the local Cartesian frames (x, y) in each region. For theoretical aims, it is sufficient to define the parametric lines α and β within these local frames. To develop a computer program for drawing of these lines, all the formulae should be referred to one global Cartesian system, e.g., to the (x, y) frame with its origin at A. The parametric lines are expressed in terms of $F_n(\alpha, \beta)$ functions, see (a.2), which are certain integrals of $G_n(\alpha, \beta)$ functions, see (a.16). Computation of the values of $F_n(\alpha, \beta)$ are much more time consuming than computation of $G_n(\alpha, \beta)$, expressed by rapidly convergent series.

The parametric lines (α, β) within $E_3E_2E_1B_1D_1OG_1B_1'E_1'E_2'C_3$ are constructed in Lewiński and Rozvany (2007). Our aim is to extend these results to the domain $C_1'G_1'O'H_1'J_1S_1ZS_1''J_1''H_1'''O'''C_1'''C_2'$, see Fig. 4.

The coordinates $x(\alpha, \beta)$, $y(\alpha, \beta)$ within ABDC domain are expressed by (II.47), (II.48). We note that (x_1, y_1) coordinates of point A are (0, 0). The (x_1, y_1) coordinates of points $\left(\widetilde{\alpha},\widetilde{\beta}\right)$ of the domain BDD_1B_1 are given by (58) of the paper mentioned above. The same (x_1, y_1) point has the coordinates (x, y) given by $x=x_1$, $y+r=y_1$; B_1 is the origin of the (x, y) frame, see Fig. 4.

6.1 Domain $B_1D_1HD_1'$

The coordinates $x(\alpha, \beta)$, $y(\alpha, \beta)$, where B_1 is the origin of the (x, y) system considered, are expressed by $\overline{x}(\alpha,\beta)$, $\overline{y}(\alpha,\beta)$ according to (II.52) or (a.58). Just the fields ($\overline{x}$, $\overline{y}$) are our convenient unknowns, since they are governed by a relatively easy set of equations (a.55) and satisfy equations of form (5.1). By using the results (II.58) one can find the boundary values of $\overline{x}$ along the lines B_1D_1' and B_1D_1

$$\begin{aligned} \frac{\overline{x}(\alpha,0)}{r} &= \sin\alpha - \cos\alpha + H_0\left(\alpha,\tfrac{\pi}{4}\right) \\ \frac{\overline{y}(0,\beta)}{r} &= \sin\beta - \cos\beta + H_0\left(\beta,\tfrac{\pi}{4}\right) \end{aligned} \tag{6.1}$$

where H_0 is defined by $(3.1)_2$. We remember that

$$\frac{\partial\overline{x}(0,\beta)}{\partial\beta} = \overline{y}(0,\beta)$$

Thus, the Riemann formula reads

$$\begin{aligned} \overline{x}(\lambda,\mu) = \overline{x}(0,0)G_0(\lambda,\mu) + \\ + \int_0^{\lambda} G_0(\lambda-\alpha,\mu)\frac{\partial\overline{x}(\alpha,0)}{\partial\alpha}d\alpha + \\ + \int_0^{\mu} G_0(\mu-\beta,\lambda)\overline{y}(0,\beta)d\beta \end{aligned} \tag{6.2}$$

substitution of (6.1) and appropriate integration gives

$$\begin{aligned} \frac{\overline{x}(\lambda,\mu)}{r} = \sin(\lambda-\mu) - \cos(\lambda-\mu) + \\ + H_0\left(\lambda,\mu+\tfrac{\pi}{4}\right) + H_1\left(\mu,\lambda+\tfrac{\pi}{4}\right) \end{aligned} \tag{6.3}$$

and $\overline{y}(\lambda,\mu) = \overline{x}(\mu,\lambda)$. Here, H_0, H_1 are defined by (3.1). To derive (6.3), one should make use of identities (a.4–a.14) and of integration rules of the Appendix. The functions $x(\lambda, \mu)$, $y(\lambda, \mu)$ can now be found by (II.52).

Having found $x(\alpha, \beta)$, $y(\alpha, \beta)$ we can draw the boundary lines: D_1H (where $\alpha = \pi/4$) and $D_1'H$ (where $\beta = \pi/4$) and obtain position of point H. The Hencky net found in $B_1D_1HD_1'$ can be extended into the adjacent domains $D_1'HH_1'O'$ and D_1OH_1H. One notes that

$$|B_1H| = \left[-1 + H_0\left(\frac{\pi}{4},\frac{\pi}{2}\right) + H_1\left(\frac{\pi}{4},\frac{\pi}{2}\right)\right]a$$

or $|B_1H| \approx 4.2195a$. Moreover,

$$|D_1D_1'| = \sqrt{2}\left[H_0\left(\frac{\pi}{4},\frac{\pi}{4}\right) + H_1\left(0,\frac{\pi}{2}\right)\right]a$$

or $|D_1D_1'| = 3.28375a$.

This domain is parameterized by $\left(\widehat{\alpha},\widehat{\beta}\right)$ such that $\widehat{\alpha}=0$ corresponds to the line D_1H. Let us take a point $M\left(\frac{\pi}{4},\beta\right)$, where $\left(\frac{\pi}{4},\beta\right)$ refer to the parameterization of $B_1D_1HD_1'$. The coordinates $x\left(\frac{\pi}{4},\beta\right)$, $y\left(\frac{\pi}{4},\beta\right)$ found above refer to (x, y) with origin at B_1. The unit vector

$$\boldsymbol{e}(\beta)=\left[\cos\left(\beta-\frac{\pi}{4}\right),\ \sin\left(\beta-\frac{\pi}{4}\right)\right] \tag{6.4}$$

of components referring to (x, y) with origin at B_1 is orthogonal to the line D_1H at point M and directed towards the domain D_1OH_1H. Let

$$\boldsymbol{r}_M(\beta)=\left[x\left(\frac{\pi}{4},\beta\right),\ y\left(\frac{\pi}{4},\beta\right)\right],\quad \boldsymbol{r}_M=\overrightarrow{B_1M}$$

and

$$\boldsymbol{r}\left(\widehat{\alpha},\widehat{\beta}\right)=\boldsymbol{r}_M\left(\widehat{\beta}\right)+\widehat{\alpha}\boldsymbol{e}\left(\widehat{\beta}\right) \tag{6.5}$$

The function $\boldsymbol{r}\left(\widehat{\alpha},\widehat{\beta}\right)$ parameterizes the lines $\widehat{\beta}=\text{const}$ and $\widehat{\alpha}=\text{const}$ within the domain considered. For $\widehat{\alpha}=r$, we obtain the parameterization of the line OH_1 and the (x, y) coordinates of point H_1. The coordinates of the Hencky net in $D_1'HH_1'O'$ are found by symmetry rules with respect to B_1H.

6.2 Domain OH_1SH_1''

The Hencky net is referred to the Cartesian system (x, y), with origin at O. We are looking for $\overline{x}(\alpha,\beta)$, $\overline{y}(\alpha,\beta)$, which fixes $x(\alpha, \beta)$, $y(\alpha, \beta)$ by (II.48). It is sufficient to find $\overline{x}(\alpha,\beta)$ since $\overline{y}(\beta,\alpha)=\overline{x}(\beta,\alpha)$. To find $\overline{x}(\alpha,\beta)$ we should have the values $\overline{x}(\alpha,0)$ (the line OH_1'') and $\overline{x}(0,\beta)$ along OH_1. We must correlate the coordinates (x, y) with origin at B_1 with the coordinates (x, y) with origin at B_1 with the coordinates (x, y) with respect to O, of the same point. Let us start with fixing the coordinates (x_0, y_0) of point O

$$\frac{x_0}{r}=\frac{3}{2}\sqrt{2}-1+\sqrt{2}\xi,\quad \frac{y_0}{r}=-1-\frac{\sqrt{2}}{2} \tag{6.6}$$

where $\xi=H_1\left(\frac{\pi}{4},\frac{\pi}{4}\right)$, in the (x, y) frame with origin at B_1. Let (x_1, y_1) be (x, y) coordinates with origin at B_1 of a certain point. Its (x, y) coordinates with respect to the (x, y) frame of origin at O are given by

$$\begin{aligned} x&=\tfrac{\sqrt{2}}{2}\left[(x_1-x_0)-(y_1-y_0)\right]\\ y&=\tfrac{\sqrt{2}}{2}\left[(x_1-x_0)+(y_1-y_0)\right]\end{aligned} \tag{6.7}$$

The formulae above determine the coordinates of points lying along OH_1 and OH_1''. This gives the formulae for $(\overline{x},\overline{y})$ coordinates of these points.

The line OH_1''

$$\begin{aligned}\frac{\overline{x}(\alpha,0)}{r}&=-(1+\xi)\cos\alpha+(2+\xi)\sin\alpha+\\&\quad+H_0\left(\alpha,\frac{\pi}{2}\right)+H_1\left(\frac{\pi}{4},\alpha+\frac{\pi}{4}\right)\\ \frac{\overline{y}(\alpha,0)}{r}&=1-(2+\xi)\cos\alpha-(1+\xi)\sin\alpha+\\&\quad+H_0\left(\frac{\pi}{4},\alpha+\frac{\pi}{4}\right)+H_1\left(\alpha,\frac{\pi}{2}\right)\end{aligned} \tag{6.8}$$

The line OH_1

$$\begin{aligned}\frac{\overline{x}(0,\beta)}{r}&=1-(2+\xi)\cos\beta-(1+\xi)\sin\beta+\\&\quad+H_0\left(\tfrac{\pi}{4},\beta+\tfrac{\pi}{4}\right)+H_1\left(\beta,\tfrac{\pi}{2}\right)\\ \frac{\overline{y}(0,\beta)}{r}&=-(1+\xi)\cos\beta+(2+\xi)\sin\beta+\\&\quad+H_0\left(\beta,\tfrac{\pi}{2}\right)+H_1\left(\tfrac{\pi}{4},\beta+\tfrac{\pi}{4}\right)\end{aligned} \tag{6.9}$$

Here (α, β) are defined within $OH_1''SH_1$. One can prove that at point O $\overline{x}(0,0)=0$, $\overline{y}(0, 0)=0$.

To find $\overline{x}$ at a point (λ, μ) we use (6.2). Substitution of (6.8), (6.9) gives

$$\begin{aligned}\frac{\overline{x}(\lambda,\mu)}{r}&=(2+\xi)\sin(\lambda-\mu)-(1+\xi)\cos(\lambda-\mu)+\\&\quad+H_0\left(\lambda,\mu+\frac{\pi}{2}\right)+H_1\left(\mu,\lambda+\frac{\pi}{2}\right)+\\&\quad+H_1\left(\mu+\frac{\pi}{4},\lambda+\frac{\pi}{4}\right)\\ \overline{y}(\lambda,\mu)&=\overline{x}(\mu,\lambda)\end{aligned} \tag{6.10}$$

The functions $x(\lambda, \mu)$, $y(\lambda, \mu)$ are then given by (a.58). Derivation of (6.10) is lengthy. It requires multiple using of properties (a.4–a.16), of the integration rule (A.7) for $S_n=F_n$ and of other integration rules reported in Lewiński et al. (1994a), Graczykowski and Lewiński (2006, 2007) and in the Appendix of the present paper.

Let us compute the distance $|OS|$. We note that $x(\theta,\theta)=\overline{x}(\theta,\theta)$, hence $|OS|=\sqrt{2}\overline{x}\left(\frac{\pi}{4},\frac{\pi}{4}\right)$ or

$$\begin{aligned}\frac{|OS|}{r}&=\sqrt{2}\left[-1-H_1\left(\tfrac{\pi}{4},\tfrac{\pi}{4}\right)+H_0\left(\tfrac{\pi}{4},\tfrac{3}{4}\pi\right)+\right.\\&\quad\left.+H_1\left(\tfrac{\pi}{4},\tfrac{3}{4}\pi\right)+H_1\left(\tfrac{\pi}{2},\tfrac{\pi}{2}\right)\right]\end{aligned} \tag{6.11}$$

or $|OS|$=10.57186a. Since $|AO|=\sqrt{2}(1+\xi)r$, we find

$$\begin{aligned}\frac{|AS|}{r}&=\sqrt{2}\left[H_0\left(\tfrac{\pi}{4},\tfrac{3}{4}\pi\right)+H_1\left(\tfrac{\pi}{4},\tfrac{3}{4}\pi\right)+\right.\\&\quad\left.+H_1\left(\tfrac{\pi}{2},\tfrac{\pi}{2}\right)\right]\end{aligned} \tag{6.12}$$

or $|AS|$=12.89382a. We compute yet $\left|H_1H_1''\right|$

$$\begin{aligned}\left|H_1H_1''\right|&=\left[\sqrt{2}+2H_0\left(\tfrac{\pi}{4},\tfrac{\pi}{2}\right)+2H_1\left(\tfrac{\pi}{4},\tfrac{3}{4}\pi\right)+\right.\\&\quad\left.+2H_1\left(\tfrac{\pi}{4},\tfrac{\pi}{2}\right)\right]r\end{aligned}$$

Or $\left|H_1H_1''\right|=8.381482a$. Hence $J_1J_1''=9.7957a$.

6.3 Domains $H_1SS_1J_1$, $H_1''SS_1''J_1''$, SS_1ZS_1''

Let us take a point M of coordinates $\left(\alpha, \frac{\pi}{4}\right)$ defined as in the previous domain. Point M lies on the H_1S curve, see Fig. 4. Its (x, y) coordinates are given by $x\left(\alpha, \frac{\pi}{4}\right)$ and $y\left(\alpha, \frac{\pi}{4}\right)$, defined as before. Thus if $\boldsymbol{r}_M = \overrightarrow{\mathrm{OM}}$, the

$$\boldsymbol{r}_M(\alpha) = \left[x\left(\alpha, \frac{\pi}{4}\right), y\left(\alpha, \frac{\pi}{4}\right)\right]$$

where (x, y) have the origin at O. The unit vector of components

$$\boldsymbol{e}(\alpha) = \left[\cos\left(\frac{\pi}{4} - \alpha\right),\ \sin\left(\frac{\pi}{4} - \alpha\right)\right] \tag{6.13}$$

referred to the same (x, y) frame is orthogonal to H_1S line at point M, directed towards the $H_1SS_1J_1$ domain. Let us introduce the mapping

$$\boldsymbol{r}\left(\widetilde{\alpha}, \widetilde{\beta}\right) = \boldsymbol{r}_M(\widetilde{\alpha}) + \widetilde{\beta}\boldsymbol{e}(\widetilde{\alpha}) \tag{6.14}$$

It determines the $\left(\widetilde{\alpha}, \widetilde{\beta}\right)$ parametric lines within the domain considered. The vector $\boldsymbol{r}(\widetilde{\alpha}, 0)$ indicates the points along J_1S_1 and, in particular, gives the coordinates of point S_1.

The net within $H_1''SS_1''J_1''$ can be found by symmetry with respect to OS.

The domain SS_1ZS_1'' is quadratic of side r. Thus, the distance between A_0 and Z equals

$$\frac{|A_0Z|}{a} = \frac{3}{2} + H_0\left(\frac{\pi}{4}, \frac{3}{4}\pi\right) + \\ + H_1\left(\frac{\pi}{4}, \frac{3}{4}\pi\right) + H_1\left(\frac{\pi}{2}, \frac{\pi}{2}\right) \tag{6.15}$$

or $|A_0Z|=14.39382a$.

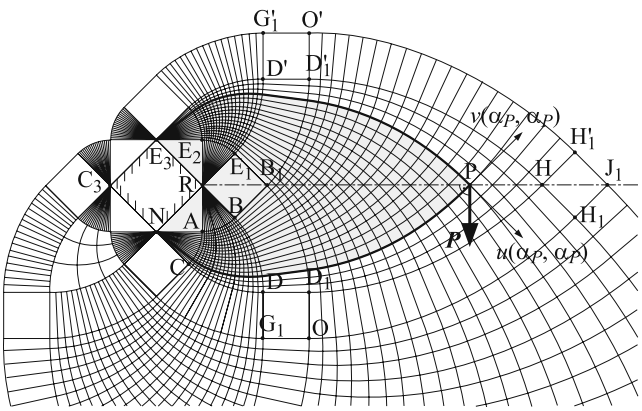

Fig. 5 Case of P between B_1 and H

7 Optimal truss volumes for special cases

The Hencky nets derived in this paper represent a class of Michell cantilevers transmitting a given point load to the edge E_3RNC_3, provided that this point load causes antisymmetric stress distribution, i.e., averaged stress distribution or distribution of force fields, see Graczykowski and Lewiński (2007, Part III).

The cases of application of the force within $O'B_1OK_1O'''C_1'''C_1'G_1'$, were discussed in Lewiński and Rozvany (2007). We shall consider now new solutions for the case of the point load applied outside the above-mentioned region.

7.1 Vertical point load between B_1 and H

Assume that the load $\boldsymbol{P}$ of magnitude P is applied at point P within $B_1D_1HD_1'$, lying between B_1 and H, see Fig. 5. Let (α_P, β_P) be (α, β) coordinates of point P, as defined within $B_1D_1HD_1'$; $0 \le \alpha_P \le \frac{\pi}{4}$. Assume for simplicity that $\boldsymbol{P}$ is directed perpendicular to B_1H.

Let the virtual displacement u_P of point P be orthogonal to B_1P, or collinear with $\boldsymbol{P}$:

$$u_P = \frac{\sqrt{2}}{2}\left(u(\alpha_P, \alpha_P) - v(\alpha_P, \alpha_P)\right) \tag{7.1}$$

or $u_P = \sqrt{2}u(\alpha_P, \alpha_P)$. By using the results (5.4), (5.6), (4.3), (4.4) we arrive at

$$\frac{u(\alpha, \alpha)}{r} = \left(2 + \frac{\pi}{2} + 4\alpha\right)G_0\left(\alpha, \alpha + \frac{\pi}{4}\right) + \\ + \left(\frac{\pi}{2} + 2\alpha\right)G_1\left(\alpha, \alpha + \frac{\pi}{4}\right) + \\ + 2\alpha G_1\left(\alpha + \frac{\pi}{4}, \alpha\right) \tag{7.2}$$

The volume V of the lightest cantilever is given by, see (a.157)

$$V = \frac{1}{\sigma_0}\boldsymbol{P} \cdot \boldsymbol{v}(\mathrm{P}) \tag{7.3}$$

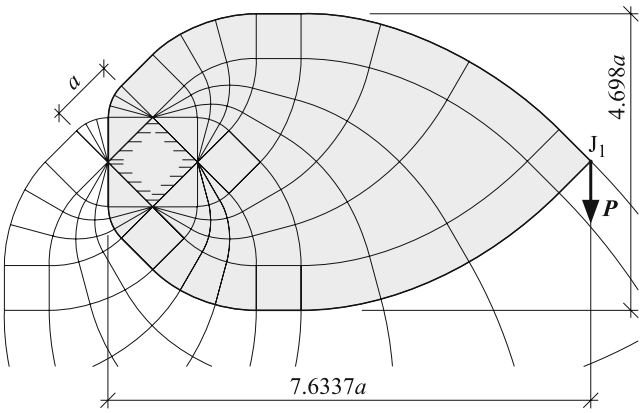

Fig. 6 Case of $P=J_1$. The ratio of the transverse to the longitudinal dimension is close to the golden section ratio and equals 0.615

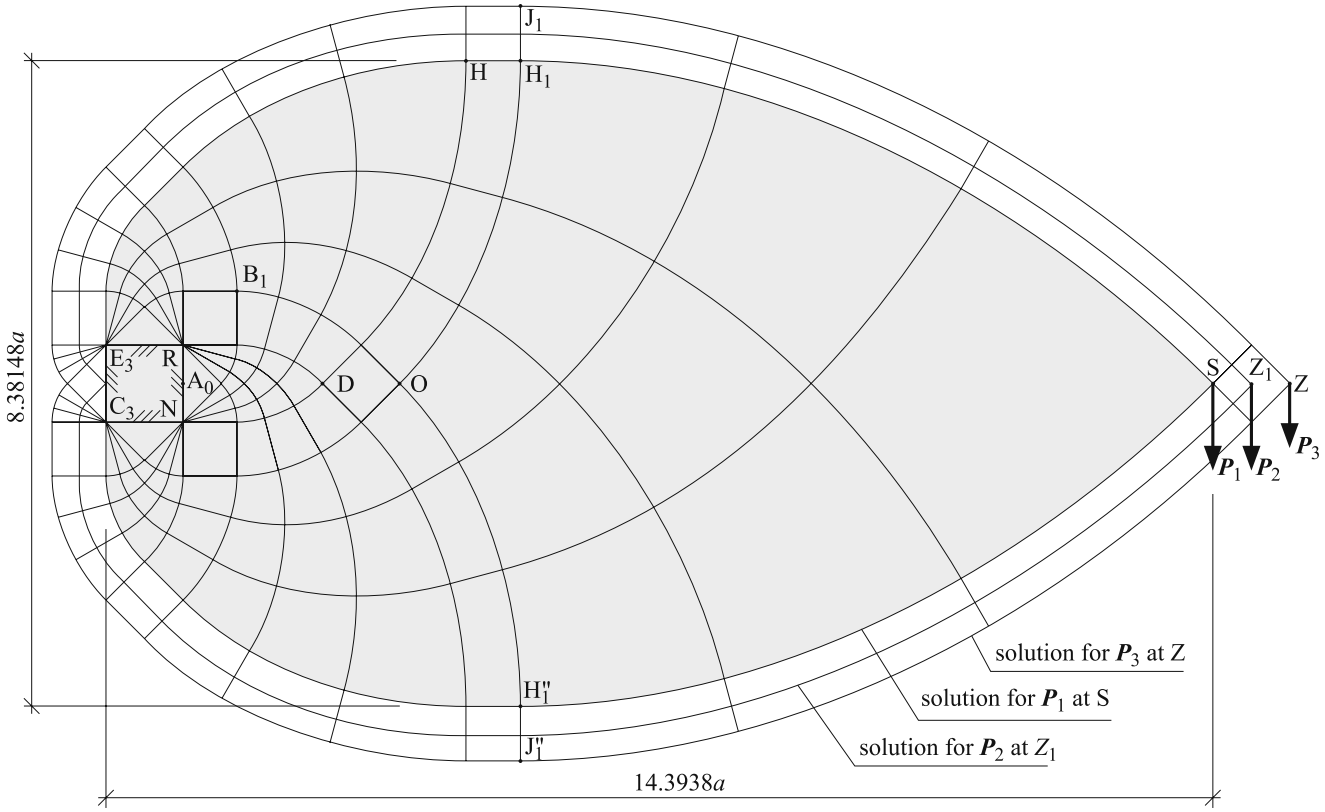

Fig. 7 Cases of P at S, Z and Z_1

where $\boldsymbol{v}$(P) is the virtual displacement vector at point P. Since $\boldsymbol{P}$ and $\boldsymbol{v}$(P) are collinear we have $V = Pu_P/\sigma_0$ or $V = (Pa/\sigma_0)\overline{V}(\alpha_P)$, where $\overline{V}(\alpha)$ is expressed by the r.h.s of (7.2). The optimal cantilever is shown in Fig. 5. If the force $\boldsymbol{P}$ is applied at B_1 the volume of the optimal structure equals $\overline{V}(0) = 2 + \pi/2$. For the case of P=H we find $\overline{V} = \overline{V}\left(\frac{\pi}{4}\right)$ or

$$\overline{V}\left(\tfrac{\pi}{4}\right) = \left(2 + \tfrac{3}{2}\pi\right) G_0\left(\tfrac{\pi}{4}, \tfrac{\pi}{2}\right) + \\ + \pi G_1\left(\tfrac{\pi}{4}, \tfrac{\pi}{2}\right) + \tfrac{\pi}{2} G_1\left(\tfrac{\pi}{2}, \tfrac{\pi}{4}\right) \tag{7.4}$$

hence $\overline{V}\left(\frac{\pi}{4}\right) = 26.59927$.

7.2 Vertical point load at J_1

Assume that $\boldsymbol{P}$ is applied at J_1, perpendicularly to B_1J_1. The virtual displacements at J_1 are given by (5.15) or $u(J_1) = (1 + C_1)r + D_1$, with C_1, D_1 given by (5.16). The volume of the optimal structure equals $V = (Pa/\sigma_0)\overline{V}$ with $\overline{V} = u(J_1)/r$ or

$$\overline{V} = \left(2 + \tfrac{3}{2}\pi\right)\left(1 + G_0\left(\tfrac{\pi}{4}, \tfrac{\pi}{2}\right)\right) + \tfrac{\pi}{2} G_1\left(\tfrac{\pi}{2}, \tfrac{\pi}{4}\right) + \\ + \pi G_1\left(\tfrac{\pi}{4}, \tfrac{\pi}{2}\right) \tag{7.5}$$

or $\overline{V} = 33.31166$. The optimal structure is shown in Fig. 6.

All edges of the square are used to support this cantilever.

7.3 Vertical point load between O and S

Let point P lie between O and S and have coordinates (α_P, β_P) within the (α, β) system. We note that the volume of Michell's structure equals $\overline{V} = (Pa/\sigma_0)\overline{V}(\alpha_P)$ with

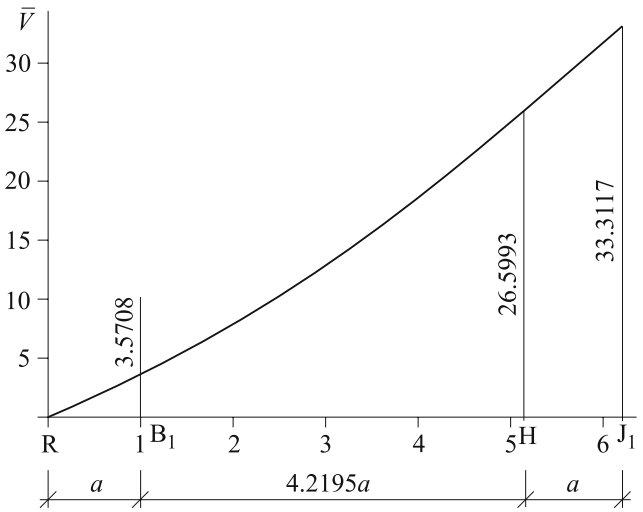

Fig. 8 Graph of $\overline{V}$ for the case of P between R and J_1

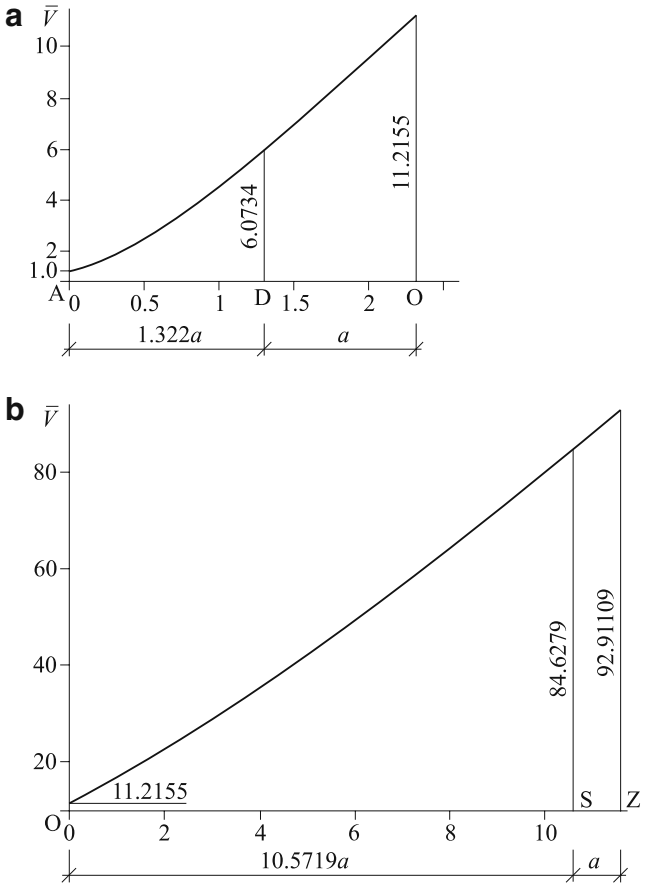

Fig. 9 Graph of $\overline{V}$ for P between: **a** A and O **b** O and Z

$\overline{V}(\alpha) = u(\alpha,\alpha)/r$ for the case of $\boldsymbol{P}$ being orthogonal to the OS line. By using (5.20) and (4.8) one finds

$$\begin{aligned}\overline{V}(\alpha) =& G_0\Big(\alpha,\alpha+\frac{\pi}{4}\Big)+\\ &+(1+\pi+4\alpha)G_0\Big(\alpha,\alpha+\frac{\pi}{2}\Big)+\\ &+\Big(1+\frac{\pi}{2}+2\alpha\Big)G_0\Big(\alpha+\frac{\pi}{4},\alpha+\frac{\pi}{4}\Big)+\\ &+(\pi+2\alpha)G_1\Big(\alpha,\alpha+\frac{\pi}{2}\Big)+\\ &+\Big(\frac{\pi}{2}+2\alpha\Big)G_1\Big(\alpha+\frac{\pi}{4},\alpha+\frac{\pi}{4}\Big)+\\ &+2\alpha G_1\Big(\alpha+\frac{\pi}{2},\alpha\Big)\end{aligned} \tag{7.6}$$

For the case of P=S we have $\alpha = \frac{\pi}{4}$ and $\overline{V} = 84.6279$. The optimal cantilever is supported on E_3RNC_3, the section E_3C_3 being not used, see Fig. 7.

7.4 Vertical point load at Z and Z_1

Let $\boldsymbol{P}$ be orthogonal to OZ and be applied at Z. The virtual displacement u at Z is given by (5.23). The volume of the optimal cantilever is $V = (Pa/\sigma_0)\overline{V}$, where $\overline{V} = u(\mathrm{Z})/r$ or

$$\begin{aligned}\overline{V} =& 2(1+\pi)+G_0\Big(\tfrac{\pi}{4},\tfrac{\pi}{2}\Big)+(1+2\pi)G_0\Big(\tfrac{\pi}{4},\tfrac{3}{4}\pi\Big)+\\ &+(1+\pi)G_0\Big(\tfrac{\pi}{2},\tfrac{\pi}{2}\Big)+\tfrac{3}{2}\pi G_1\Big(\tfrac{\pi}{4},\tfrac{3}{4}\pi\Big)+\\ &+\pi G_1\Big(\tfrac{\pi}{2},\tfrac{\pi}{2}\Big)+\tfrac{\pi}{2}G_1\Big(\tfrac{3}{4}\pi,\tfrac{\pi}{4}\Big)\end{aligned} \tag{7.7}$$

hence $\overline{V} = 92.911089$.

We see that the interior of the support on E_3C_3 is not used. If the force is applied in the middle of SZ or at Z_1, then the supporting bars start from the middle of E_3C_3, see Fig. 7. The results of sections 7.1–7.4 are shown graphically in Figs. 8 and 9.

7.5 Comparison with volumes of the cantilevers supported on a circle

The lightest cantilever supported on a circle has been found by Michell (1904). If the radius of the circle equals b, then the volume of the optimal cantilever corresponding to the force $\boldsymbol{P}$ orthogonal to its symmetry axis equals

$$V_c = \frac{Pa}{\sigma_0}\left(2\frac{L}{a}\ln\left(\frac{L}{a}\frac{a}{b}\right)\right) \tag{7.8}$$

where L is the distance of point P to the center of the circle.

Let us now approximate the previous results by cantilevers supported on an equivalent circle of center at T. We choose the radius b of the equivalent circle in two manners, by assuming

1. the area of the circle of radius b equals the area of the square $a\times a$. Then $a = \sqrt{\pi}b$ and $V_c = (Pa/\sigma_0)\overline{V}_{c1}$

Table 1 Volumes of Michell's cantilevers supported on the $a\times a$ square and on the circles of radii b such that $a/b = \sqrt{\pi}, \frac{\pi}{2}$

Point P	A	B_1	D	O	H	J_1	S	Z
$\xi = L/a$	1.0	1.7071	2.322	3.322	5.9266	6.9266	13.8938	14.8938
$\overline{V}$	1.0	3.5708	6.074	11.2155	26.5993	33.3117	84.6279	92.9112
$\overline{V}_{c1}$, $a = \pi^{\frac{1}{2}}b$	1.1447	3.7801	6.5703	11.7794	27.8765	34.7401	89.0261	97.5040
$100\%(\overline{V}-\overline{V}_{c1})/\overline{V}$	−14.47%	−5.86%	−8.17%	−5.03%	−4.80%	−4.29%	−5.20%	−4.94%
$\overline{V}_{c2}$, $a = \pi b/2$	0.903	3.3677	6.0094	10.9769	26.4448	33.0629	85.6699	93.9062
$100\%(\overline{V}-\overline{V}_{c2})/\overline{V}$	−9.68%	−5.69%	−1.06%	2.13%	0.58%	0.75%	−1.23%	−1.07%

The force is applied at points A, B, D, O, H, J_1, S, Z in a locally antisymmetric manner

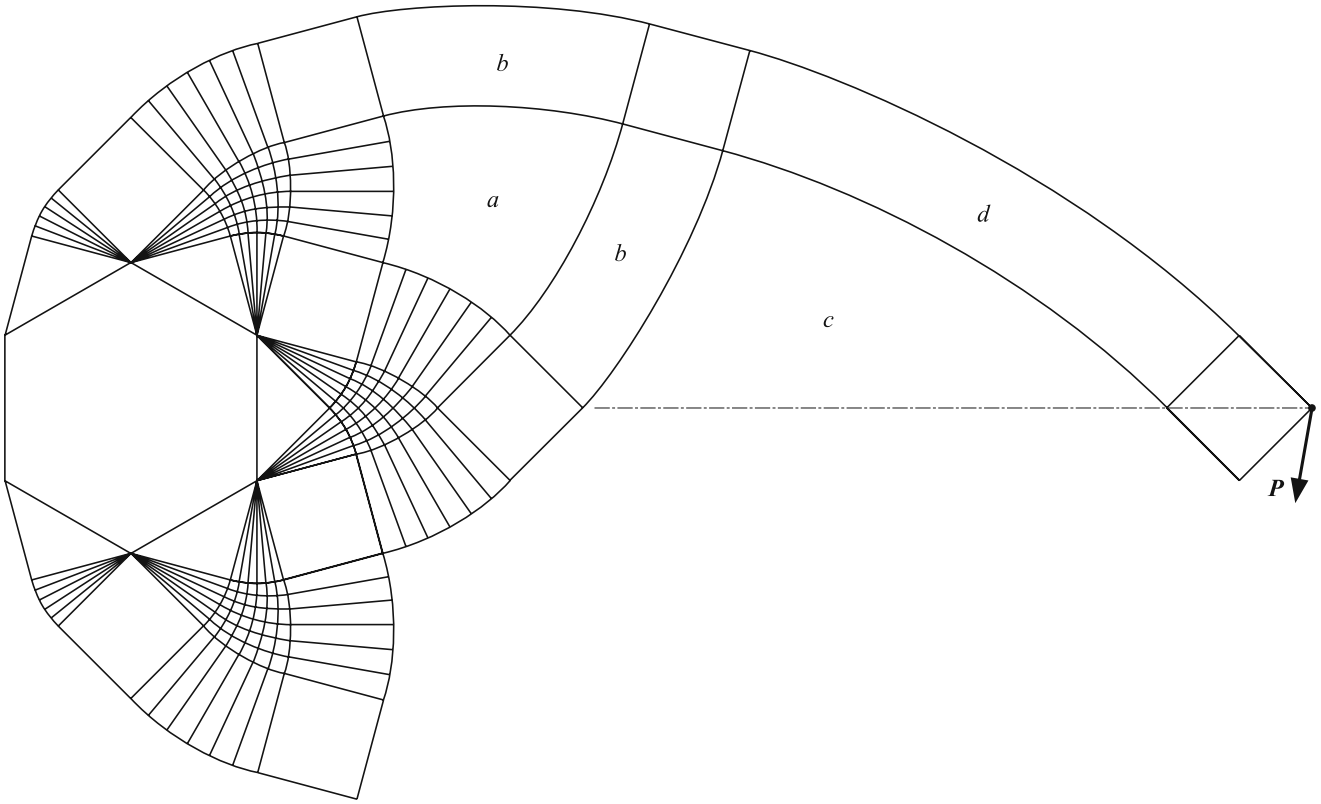

Fig. 10 Optimal topology for a regular hexagonal support

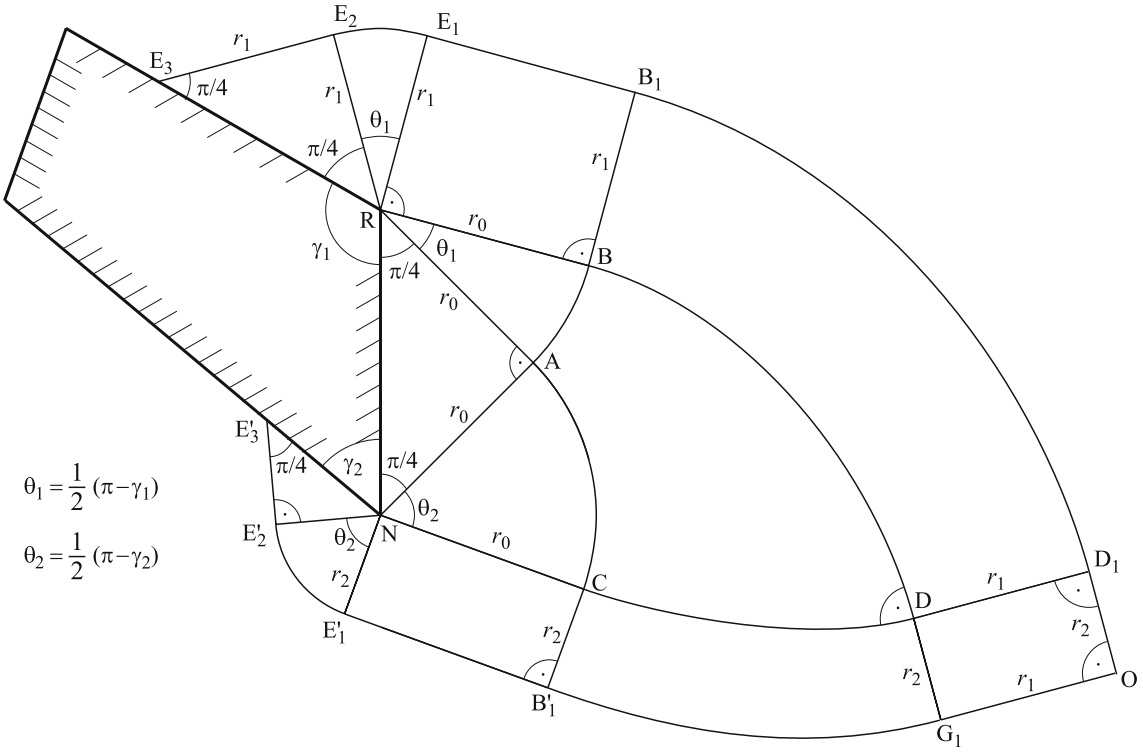

Fig. 11 Optimal topology for an irregular polygonal support

2. the perimeter of the circle of radius b equals the perimeter of the square $a\times a$.

Then $a=\frac{\pi b}{2}$ and $V_c=\left(Pa/\sigma_0\right)\overline{V}_{c2}$
Thus, we have

$$\overline{V}_{c1}=2\xi\ln\left(\sqrt{\pi}\xi\right),\quad \overline{V}_{c2}=2\xi\ln\left(\frac{\pi\xi}{2}\right) \tag{7.9}$$

where $\xi=L/a$, $L=|\mathrm{TP}|$, T being the center of the circle and of the square.

We note that $\overline{V}_{c1}$ overestimates the value $\overline{V}$, see Table 1. The volume $\overline{V}_{c2}$ assumes values close to $\overline{V}$ and only slightly smaller than $\overline{V}$, if the point P lies on the diagonal of the supporting square. Note that the smaller b the greater V_c. Since the circle (2) is greater than the circle (1), we have $\overline{V}_{c1}>\overline{V}_{c2}$ in all cases. However, only for two cases: P=H and P=J_1 the estimates $\overline{V}_{c2}<\overline{V}<\overline{V}_{c1}$ hold good. The choice of the circle inscribed in the square $(b=a/2)$ leads to a further overestimate of V.

7.6 Brief outline of a proof that the optimal Michell topology for a regular polygonal support tends to that for a circular support when the number of sides of the polygon approaches infinity

The solution for a circular support can be found in Hemp (1973, Section 7.3). Assume that A_1, A_2, ..., A_n are vertices of the polygon support, lying on the given circle. Let B_n be vertices of right-angle triangles of equal sides $|\mathrm{A}_n\mathrm{B}_n|=|\mathrm{A}_{n+1}\mathrm{B}_n|$ such that B_n lie outside the polygon and

$$\angle(\mathrm{B}_n\mathrm{A}_n\mathrm{A}_{n+1})=\frac{\pi}{4},\quad \angle(\mathrm{B}_n\mathrm{A}_{n+1}\mathrm{A}_n)=\frac{\pi}{4} \tag{7.10}$$

An example of such triangles can be seen in Fig. 10. If n tends to infinity then $\angle(\mathrm{B}_n\mathrm{A}_{n+1}\mathrm{B}_{n+1})\to\pi/2$, which means that the fan regions (see again Fig. 10) between B_n, A_{n+1}, B_{n+1} disappear. Moreover, since the side length of the polygonal support approaches zero, the side length of the triangles and of the empty square regions, as well as the width of the regions with unidirectional fibers (cf. Fig. 10) will also approach zero. The lines α=const, β=const become tangent to $\mathrm{B}_n\mathrm{A}_n$, $\mathrm{B}_n\mathrm{A}_{n+1}$ and with the circle they enclose an angle $\pi/4$.

Due to rotational symmetry of the problem for n tending to infinity, the Lamé fields A and B cannot depend on $\beta-\alpha$; they depend only on $\alpha+\beta$, i.e., $A=f(\alpha+\beta)$. Application of Eq. (a.52) leads to the solution composed of logarithmic spirals, see section 4.6 in Hemp (1973), which results in the known Michell solution for the exterior of the circle.

8 Concluding remarks: further extensions

Using the procedure demonstrated in this paper, optimal Michell topologies can also be derived readily for

1. square supports and loads at a greater distance than the one in Fig. 1,
2. any convex polygonal support.

For a regular hexagonal support, for example, the optimal region topology is shown in Fig. 10. The optimal geometry of the regions on the left side of Fig. 10 can be taken from Fig. 5 of the paper by Lewiński and Rozvany (2007). The exact geometry would have to be derived only for regions “a” through “d” in Fig. 10, by the method already used previously.

The reader may pose the question, how to handle nonregular convex polygonal supports? The answer is relatively simple.

Unequal angles between sides is not a problem, this only causes circular fans of differing angular width in the solution. To see this, we may compare Figs. 1 and 10. If the sides of the polygonal support are of unequal lengths, then the triangular regions become of unequal size, and the square regions for regular polygons become rectangular for irregular ones. The above features of Michell layouts for nonregular polygonal supports are illustrated with the optimal region topology in Fig. 11, for which the optimal geometry has not been derived yet.

Acknowledgement The work was partially supported within the grant 4T07A 038 30 of the Polish Ministry of Science and Higher Education: *Theory and numerical implementation of relaxed formulations of optimization problems with coupled fields. Designing of the layout of materials in the composite structures* and by OTKA (Hungary), grant No. K62555. The technical help of Mrs Iwona Malicka is highly acknowledged.

Appendix

By applying the Laplace transform method, see (a.28, a.29), one can find

$$\int_0^\lambda G_0(\lambda-\alpha,\mu)G_1(\theta,\alpha)d\alpha= \tag{A.1}$$
$$G_0(\lambda,\mu+\theta)-G_0(\lambda,\mu)$$

$$\int_0^\lambda G_0(\lambda-\alpha,\mu)F_n(\alpha,\theta)d\alpha=F_{n+1}(\lambda,\mu+\theta) \tag{A.2}$$

where θ is arbitrary and $n\geq 0$.

Due to symmetry of convolution in (a.16), one finds

$$\int_0^{\lambda} G_0(\lambda-\alpha,\mu)\cos\alpha\, d\alpha = F_1(\lambda,\mu) \tag{A.3}$$

$$\int_0^{\lambda} G_0(\lambda-\alpha,\mu)\sin\alpha\, d\alpha = F_2(\lambda,\mu) \tag{A.4}$$

Let S_n stand for G_n or F_n. Let

$$N_1 = \int_0^{\lambda} G_0(\lambda-\alpha,\mu)S_{n-1}(\alpha+\theta,\theta)d\alpha \tag{A.5}$$

$$N_2 = \int_0^{\mu} G_0(\mu-\beta,\lambda)S_{n+1}(\theta,\beta+\theta)d\beta \tag{A.6}$$

Then for arbitrary integer n and $\theta \in \mathbb{R}$ one obtains

$$N_1 + N_2 = S_n(\lambda+\theta,\mu+\theta) - S_n(\theta,\theta)G_0(\lambda,\mu) \tag{A.7}$$

by using (a.23). The results for N_1 and N_2, separately, are unknown.

References

Allaire G, Jouve F (2006) Coupling level set method and topological gradient in structural optimization. In: Bendsøe MP, Olhoff N, Sigmund O (eds) Proc IUTAM Symp. on Topological Design Optimization of Structures, Machines and Materials (Copenhagen). Springer, Dordrecht, pp 3–12

Chan HSY (1963) Optimum Michell frameworks for three parallel forces. The College of Aeronautics. Cranfield, Report AERO No 167

Chan HSY (1964) Tabulation of some layouts and virtual displacement fields in the theory of Michell optimum structures. The College of Aeronautics. Cranfield, CoA Note Aero No 161

Chan HSY (1967) Half-plane slip-line fields and Michell structures. Q J Mech Appl Math 20:453–469

Chan HSY (1975) Symmetric plane frameworks of least weight. In: Sawczuk A, Mróz Z (eds) Optimization in structural design. Springer, Berlin, pp 313–326

Graczykowski C, Lewiński T (2005) The lightest plane structures of a bounded stress level, transmitting a point load to a circular support. Control Cybern 34:227–253

Graczykowski C, Lewiński T (2006) Michell cantilevers constructed within trapezoidal domains. Part I: Geometry of Hencky nets. Struct. Multidisc. Optim. 32, 347–368. Part II: Virtual displacement fields, ibidem 32, 463–471

Graczykowski C, Lewiński T (2007) Michell cantilevers constructed within trapezoidal domains. Part III: Force fields, Struct. Multidisc. Optim. 33, 27–46. Part IV: Complete exact solutions of selected optimal designs and their approximations by trusses of finite number of joints, ibidem 33, 113–129

Hemp WS (1973) Optimum structures. Oxford Clarendon Press, Oxford

Lewiński T, Rozvany GIN (2007) Exact analytical solutions for some popular benchmark problems in topology optimization II: three-sided polygonal supports. Struct Multidisc Optimiz 33:337–349

Lewinski T, Rozvany GIN (2008) Exact analytical solutions for some popular benchmark problems in topology optimization III: L-shaped domains. Struct Multidisc Optim (published online)

Lewiński T, Zhou M, Rozvany GIN (1994a) Extended exact solutions for least-weight truss layouts – Part I: cantilever with a horizontal axis of symmetry. Int J Mech Sci 36:375–398

Lewiński T, Zhou M, Rozvany GIN (1994b) Extended exact solutions for least-weight truss layouts—Part II: unsymmetric cantilevers. Ibidem 399–419

Michell AGM (1904) The limits of economy of material in frame-structures. Phil Mag 8:589–597

Prager W, Rozvany GIN (1977) Optimization of structural geometry. In: Bednarek AR, Cesari L (eds) Dynamical systems. Academic, New York

Rozvany GIN (1998) Exact analytical solutions for some popular benchmark problems in topology optimization. Struct Multidisc Optimiz 15:42–48

Rozvany GIN, Gollub W (1990) Michell layouts for various combinations of line supports, Part I. Int J Mech Sci 32:1021–1043

Rozvany GIN, Bendsøe MP, Kirsch U (1995) Layout optimization of structures. Appl Mech Rev 48:41–119

Rozvany GIN, Gollub W, Zhou M (1997) Exact Michell trusses for combinations of line supports, Part II. Struct Optim 14: 138–149